19

The effect of nanoparticles on the generation characteristics of an aqueous solution of rhodamine 6G. Magnetic field control capabilities

© M.G. Kucherenko[1], V.M. Nalbandyan[1], I.R. Alimbekov[2]

[1] Center of Laser and Information Biophysics, Orenburg State University, Orenburg, Russia
[2] Collective Use Center for Instrumentation „Institute of Micro- and Nanotechnology", Orenburg State University, Orenburg, Russia

e-mail: clibph@yandex.ru

Received May 13, 2025
Revised November 10, 2025
Accepted November 12, 2025

The effect of dielectric and conductive nanoparticles on the threshold of generation of an aqueous solution of rhodamine 6G has been experimentally investigated. It has been established that an increase in the volume fraction of nanoparticles in solution leads to a decrease in the generation threshold to a certain limit, after which its increase is observed. The magnitude of this effect is 30–60 %, depending on the material of the nanoparticles. The problem of magnetic control of the laser generation threshold by introducing magnetized metal nanoparticles into the active medium is considered. A mathematical model of a single-mode laser with three-level atoms of an active medium and spherical plasmon reflectors embedded in it is presented. Analytical expressions for the threshold of laser generation with characteristic dependences on magnetic field induction for conductive diamagnetic nanoparticles are obtained and analyzed.

Keywords: generation threshold, spherical nanoparticle, magnetic field, stimulated radiation.

DOI: 10.61011/EOS.2025.11.62924.8166-25

Introduction

In recent years, problems of improving the characteristics of laser radiation generation have attracted significant interest due to the wide application of laser emitters in optoelectronics and medical diagnostics. Light generation is observed in various organic and inorganic materials, such as photonic crystals, quantum dots, metallic nanoparticles (NPs), dye solutions, and others.

A large number of works can be found in which the authors investigate the generation characteristics of laser dyes with the addition of such particles as semiconductor ZnO NPs [1–5], dielectric (SiO_2) [6,7], as well as NPs from some other materials [8,9]. These works demonstrate that combining an organic dye (rhodamine) with NPs improves the output parameters of laser radiation. In work [7], it was established that the size and concentration of silica dioxide particles affect the characteristics of a random laser. It is also noted that SiO_2 NPs contribute to much slower photodegradation of dye molecules compared to titanium dioxide NPs.

The efficiency of random lasers can be enhanced by adding plasmonic NPs from noble metals to the active medium, as done in studies [10,11], and bimetallic NPs with a silver/gold structure [12,13]. Such NPs significantly enhance electromagnetic fields due to localized plasmonic oscillations, which in turn increases the efficiency of random laser generation. In [10], plasmonic thin-film lasers based on gold NPs deposited on a glass substrate are reported. Such laser geometry leads to an increase in radiation intensity and a decrease in the generation threshold. Works exist where NPs in the form of flowers [14] and triangles [15] are used as plasmonic amplifiers for dye generation.

In a series of works by the authors' team [16–18], a physical interpretation is given for the experimentally observed substantial decrease in the superluminescence threshold and short-wavelength shift of the stimulated emission spectrum maximum in a rhodamine 6G (R6G) solution with agglomerated silver NPs. The authors explain this effect by significant local enhancement of the optical pumping field near the complex surface of nanostructured aggregates. In [16], it is shown that using gold, silver, platinum, or zinc oxide NPs results in approximately equal threshold values at the same NP concentrations.

To explain the experimental results on the decrease in the dye generation threshold upon adding silver NPs, the authors of work [19] considered a simple model of spontaneous and stimulated emissions from dye molecules located in the near field of plasmonic NPs. Theoretical studies of a random laser formed from an optically transparent medium and scattering activated NPs are conducted [20]. In another work, a similar effect is observed when studying a flat disk made from zinc oxide powder [21]. In [22], the characteristics of a random laser are theoretically and numerically calculated, and a more rigorous model describing photon motion in a scattering medium is proposed. The authors claim that the classical diffusion model poorly describes photon dynamics.

Another method for controlling the dye generation threshold could be the influence of a constant magnetic field on a hybrid system consisting of an emitter and plasmonic NPs of spherical or spheroidal shape. As shown in works [23,24], a magnetic field allows modulation of the luminescent signal of such nanosystems.

The study of dye generation properties finds application in optoelectronics, sensing, and solar energy. In [25], a white random laser (White-RL) with high purity and stability, using organic laser dyes, is demonstrated. The use of zinc oxide-based laser systems is promising in photocatalysis and opens new opportunities for improving solar cell production technologies and environmentally friendly catalysts in chemical processing [26].

In the present work, it is experimentally shown that adding NPs of various natures to an aqueous rhodamine 6G solution contributes to a decrease in the generation threshold within a certain range of NP concentrations. Additionally, the influence of an external constant magnetic field on the generation threshold parameters of a dye with conductive NPs in the active medium is theoretically investigated.

Experimental part

Materials and methods

Spherical NPs from different materials were synthesized chemically. The following substances were used: deionized water, ethyl alcohol, tetraethoxysilane (TEOS), zinc nitrate, potassium hydroxide 89.9 %, cobalt chloride, hydrazine hydrate, silver nitrate, sodium citrate.

Synthesis of SiO_2 NPs was carried out using the Stöber method [27]. It includes stages of hydrolysis and condensation. Using this method, SiO NPs with sizes of 400 ± 80 nm were synthesized. ZnO NPs were obtained in two stages according to the procedure described in work [28]. The diameter of the obtained NPs was 70 ± 5.5 nm. Synthesis of Co NPs was performed by chemical precipitation with reduction from cobalt chloride using hydrazine hydrate [29]. The diameter of the obtained NPs was 70 ± 4 nm. The colloidal solutions of the synthesized NPs described above were subjected to heat treatment to obtain a stable powder, which was subsequently diluted in distilled water in the required proportions. Ag NPs were synthesized by the citrate method (Turkevich-Frens method). As a result, a homogeneous colloidal solution of silver NPs with an average diameter of 57 ± 25 nm was obtained.

The choice of Ag, Co, ZnO, and SiO_2 was due to the need to investigate the combined influence of plasmonic, magnetic, and dielectric factors on rhodamine 6G laser generation processes. Silver NPs provide local enhancement of the electromagnetic field due to surface plasmon resonance, which can contribute to increased generation intensity. Cobalt NPs contribute to the magnetic response of the system and allow evaluation of the external magnetic field influence within the Drude model framework. ZnO NPs, with their semiconductor properties, alter energy transfer between the dye and nanostructures, while SiO NPs serve as a dielectric comparison medium without contributing plasmonic or magnetic effects.

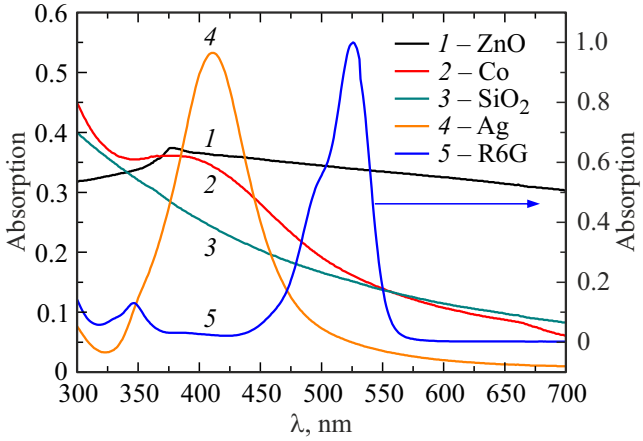

Figure 1. Absorption spectra of colloidal solutions of synthesized NPs and R6G dye. *1* — ZnO, *2* — Co, *3* — SiO_2, *4* — Ag, *5* — R6G.

Particle sizes were measured by dynamic light scattering on a Malvern Zetasizer Ultra photocorrelator. Synthesis of NPs and measurement of their sizes were performed using equipment of the Collective Use Center „Institute of Micro- and Nanotechnology“ of Orenburg State University.

Absorption spectra of NP colloidal solutions were measured on a T-70 spectrophotometer. The absorption maximum for silver NPs was $\lambda = 411$ nm for zinc oxide — $\lambda = 377$ nm (Fig. 1). Cobalt and silicon particles showed no pronounced absorption maximum.

Samples for investigation were prepared as follows: 10 mg of the obtained NP powder were diluted in 10 mL of distilled water and placed in an ultrasonic bath until a homogeneous solution was obtained. An aqueous solution of Rhodamine 6G with a concentration of $C = 10^{-4}$ mol/L was supplemented with an equal volume of a mixture of distilled water and diluted NP to maintain the dye concentration in the investigated sample at $C = 4 \cdot 10^{-5}$ mol/L.

For each type of NP, six samples were prepared with different volume fractions of ν_{NP} NP in the total solution:

1) to 1.2 mL R6G were added 0.04 mL NP and 1.96 mL distilled water; thus, the total sample volume was 3.2 mL with a NP volume fraction of 1.25 %;

2) to 1.2 mL R6G were added 0.06 mL NP and 1.94 mLH_2O; for this sample, the NP volume fraction was 1.87 %;

3) 0.1 mL NP — 3.12 %;

4) 0.3 mL NP — 9.4 %;

5) 1 mL NP — 31.2 %;

6) 2 mL NP — 62.4 %;

7) the baseline solution for comparison was obtained by mixing 1.2 mL R6G and 2 mL distilled water.

The registration of emission spectra of the R6G solution was performed using an experimental setup schematically

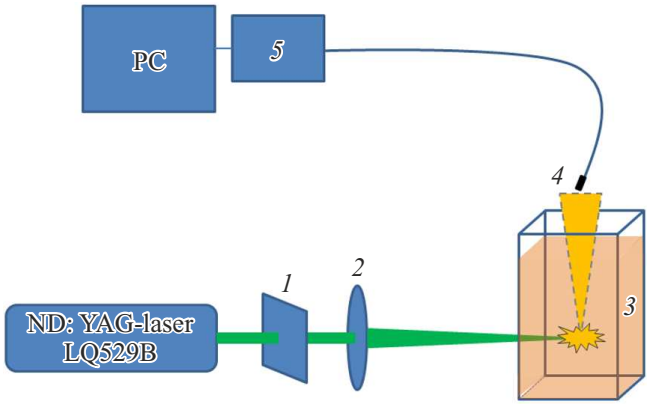

Figure 2. Schematic of the experiment. *1* — filter, *2* — collecting lens, *3* — cuvette with solution, *4* — optical fiber, *5* — CCD spectrometer BIM-6002A.

shown in Fig. 2. Optical pumping of the dye solution was carried out with pulses of the second harmonic ($\lambda = 532$ nm) of an Nd:YAG laser LQ529B with a duration of 10 ns. The pump laser energy of E varied in the range from 2 to 36 mJ by adjusting the interval between pulses. The resulting emission in the solution was directed into an optical fiber positioned above the cuvette. The signal was then transmitted via the optical fiber to the CCD spectrometer BIM-6002A, synchronized with the pump laser.

Results and discussion

Within the framework of this study, a series of experiments was conducted to measure the luminescence spectra of samples at varying pump energies of E. Both the type of added NP and their volume fraction in the dye solution were varied during the investigation.

The emission spectrum of the dye solution becomes distorted upon reaching a certain pump energy — a narrow peak appears at the spectrum maximum, which is a consequence of dye lasing (stimulated emission) (Fig. 3). For the dye solution without NP ($\nu_{NP} = 0\,\%$) lasing is observed at $E = 12$ mJ (Fig. 3, *a*). The addition of NP reduces the lasing threshold by 30 % to $E = 8$ mJ in the case of Ag and Co NP ($\nu_{NP} = 1.25\,\%$). ZnO NP at the same volume fraction reduced the lasing threshold by 60 %, with the narrow peak appearing at $E = 4$ mJ.

At low pump energies, the registered spectrum corresponds to spontaneous emission, with the emission maximum wavelength at 565 nm. Upon increasing the pump energy, when dye lasing occurs, the emission maximum wavelength shifts to the shorter-wavelength region of the spectrum to ≈ 557 nm. This shift of the emission maximum to the blue region of the spectrum is observed independently of the NP material.

The addition of any NP at a volume fraction of 1.25 % to the R6G solution leads to a reduction in the lasing threshold. Upon gradually increasing the NP fraction to 3.12–9.4 % the lasing threshold remains unchanged, but further increase in NP concentration leads to its rise. From Fig. 4, *a*, it follows that lasing is observed over a broader range of concentrations without change in the threshold value when using dielectric SiO_2 particles. In the case of silver or zinc oxide NP, lasing ceases upon reaching a volume fraction of $\nu_{NP} = 9.4\,\%$.

In investigating the dependence of emission spectrum amplitude on NP volume fraction, an initial increase in spectrum intensity is observed due to enhanced dye lasing (Fig. 4, *b*). Thus, adding Ag NP at $\nu_{NP} = 1.25\,\%$ increases the solution glow intensity by a factor of 2, Co NP at $\nu_{NP} = 9.4\,\%$ — by a factor of 1.5, SiO_2 NP at $\nu_{NP} = 31.2\,\%$ — by a factor of 2.4, ZnO NP at $\nu_{NP} = 9.4\,\%$ — by a factor of 2.5. Further increase in the NP fraction in the solution leads to luminescence quenching and a decrease in spectrum amplitudes.

The most appropriate explanation for the influence of NP on the dye lasing threshold can be found within the framework of two different assumptions.

Action of the plasmonic mechanism (for conducting NP). The near field of plasmonic NP is enhanced by several orders of magnitude compared to the incident field. Dye molecules entering this region emit much more efficiently.

Emergence of a random laser regime. A photon emitted by an excited molecule is multiply scattered by NP and returns to the pump beam excitation region, contributing to stimulated emission. Upon reaching certain values of optical pump energy density, the spectral width of secondary emission in such objects sharply narrows, and the pulse duration substantially decreases.

Theoretical Model of the Influence of Magnetic Field on the Lasing Threshold of Systems with Plasmonic NP

Plasmonic NP influence the laser generation process by affecting two independent channels of energy transformation in three-level atoms (TLA) of the active medium: radiative and nonradiative. The efficiency of the first channel changes in the presence of NP due to the induced additional dipole moment in it from the polarization by the field of the activated TLA [30]. Nonradiative TLA decay becomes more probable upon approaching the NP due to energy transfer to the metal with simultaneous generation of a localized plasmon [23]. The magnetization of the conductor's electron plasma in a field with induction **B** leads to a change in the electric polarizability $\alpha(\omega)$ of the NP and its dielectric permeability $\varepsilon(\omega)$ which depend on the frequency ω of the electromagnetic field.

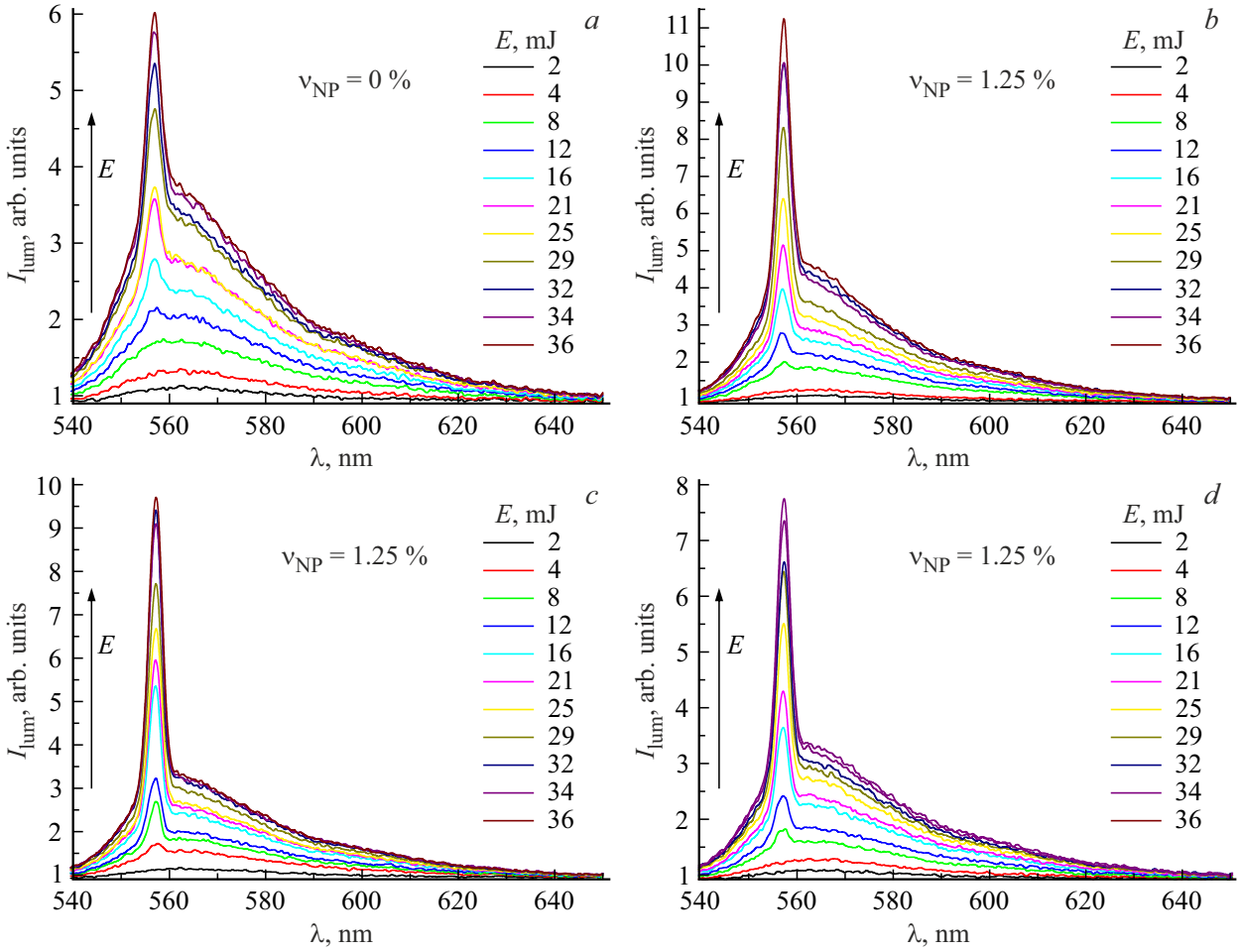

Figure 3. Luminescence and lasing spectra of R6G solution (*a*), with added Ag NP (*b*), ZnO (*c*), Co (*d*).

The tensor $\overleftrightarrow{\varepsilon}_1(\omega|\mathbf{B})$ of the dielectric permeability of a metal with magnetized electron plasma has the form [23]

$$\overleftrightarrow{\varepsilon}_1(\omega|\mathbf{B}) = \begin{pmatrix} \varepsilon_\perp(\omega|\mathbf{B}) & ig(\omega|\mathbf{B}) & 0 \\ -ig(\omega|\mathbf{B}) & \varepsilon_\perp(\omega|\mathbf{B}) & 0 \\ 0 & 0 & \varepsilon_\parallel(\omega) \end{pmatrix}, \quad (1)$$

$$\varepsilon_\perp = \varepsilon_\infty - \frac{\omega_p^2(\omega + i\gamma)}{\omega[(\omega + i\gamma)^2 - \Omega_L^2]}, \quad \varepsilon_\parallel = \varepsilon_\infty - \frac{\omega_p^2}{\omega(\omega + i\gamma)},$$

$$g = \frac{\omega_p^2 \Omega_L}{\omega[(\omega + i\gamma)^2 - \Omega_L^2]}. \quad (2)$$

The gyration vector g determines the off-diagonal elements of the dielectric permeability tensor: $\varepsilon_{xy} = -\varepsilon_{yx} = ig$. The parameters $\omega_p = \sqrt{4\pi e^2 n_e/m}$ and $\Omega_L = eB/m^*c$ in (1) and (2) — plasma (Langmuir) and Larmor frequencies of electrons, respectively, γ — electron collision frequency (dissipation coefficient).

In the case of uniform spherical particles of radius R made of a conducting material with dielectric permeability $\overleftrightarrow{\varepsilon}_1(\omega|\mathbf{B})$ their dipole dynamic polarizability $\alpha(\omega|\mathbf{B})$ in a magnetic field of induction $\mathbf{B}$ and in a nondispersive dielectric medium with permeability ε_2 takes the following tensor form [31]:

$$\overleftrightarrow{a}(\omega|\mathbf{B}) = R^3\left[\varepsilon_1(\omega|\mathbf{B}) - \varepsilon_2\overleftrightarrow{\mathbf{I}}\right]\left[\varepsilon_1(\omega|\mathbf{B}) + 2\varepsilon_2\overleftrightarrow{\mathbf{I}}\right]^{-1}. \quad (3)$$

The rate of nonradiative energy transfer of electronic excitation from the molecule to the metallic NP is identified with the rate of energy dissipation from a point dipole source in the NP volume and can be written as [31]

$$U(\mathbf{r}_0|\mathbf{B}) = \frac{1}{2\hbar}\,\mathrm{Im}\left[\mathbf{p}\overleftrightarrow{G}(\mathbf{r}_0)\overleftrightarrow{\alpha}(\omega|\mathbf{B})\overleftrightarrow{G}(\mathbf{r}_0)\mathbf{p}\right]. \quad (4)$$

Here, $\mathbf{p}$ — transition dipole moment of the molecule, $\overleftrightarrow{G}(\mathbf{r}_0) = r_0^{-3}(3\mathbf{n}\otimes\mathbf{n} - \overleftrightarrow{\mathbf{I}})$ — quasistatic dyadic Green's function of the point dipole source, $\overleftrightarrow{\mathbf{I}}$ — second-rank unit matrix, r_0 — distance between the molecule and the NP center.

The expression for the rate w_{sp} of spontaneous recombinational glow of a molecule located near the NP at a distance r_0 from its center, in the presence of an external magnetic field, takes the following form [31]:

$$w_{sp}(\mathbf{r}_0|\mathbf{B}) = \frac{4}{3}\frac{\omega^3}{\hbar c^3}\left|\left[\overleftrightarrow{\mathbf{I}} + \overleftrightarrow{G}(\mathbf{r}_0)\overleftrightarrow{\alpha}(\omega|\mathbf{B})\right]\mathbf{p}\right|^2. \quad (5)$$

The photon rate equations and population inversion for three-level atoms (balance equations) have the form [32]

$$\dot{n} = -2bNn + \gamma_{\parallel}(n^{(0)} - n),$$
$$\dot{N} = -2\kappa N + bV_a nN, \quad (6)$$
$$\gamma_{\parallel} = \frac{W_{\text{pump}}T_1 + 1}{T_1}, \; n^{(0)} = \frac{W_{\text{pump}}T_1 - 1}{W_{\text{pump}}T_1 + 1}\, n_0,$$
$$\frac{1}{T_1} = w_{\text{sp}}(\mathbf{r}_0|\mathbf{B}) + U(\mathbf{r}_0|\mathbf{B}), \; b = \sigma c/V,$$

where n_0 — molecule concentration, n — population inversion, N — number of photons in the resonator, V_a — resonator mode volume, κ — photon decay rate in the resonator, W_{pump} — pump rate, b — coefficient proportional to the stimulated transition rate involving a photon, σ — photon absorption cross-section by TLA, V — effective resonator mode volume.

The pump rate upon light excitation with intensity I

$$W_{\text{pump}} = \frac{4\pi^2|\mathbf{P}_{\text{eff}}|^2 I \cdot \cos^2\beta}{\sqrt{\varepsilon_2}\hbar^2 c}\,\delta(\omega - \omega_0), \quad (7)$$

where ω, c — frequency and speed of the exciting light, $\mathbf{P}_{\text{eff}} = [\overleftrightarrow{\mathbf{I}} + \overleftrightarrow{G}(\mathbf{r}_0)\overleftrightarrow{\alpha}(\omega|\mathbf{B})]\mathbf{p}$, $\mathbf{p}$ — transition vector dipole moment in TLA at frequency ω_0; ε_2 — dielectric permeability of the active medium with non-activated TLA, β — angle between the transition dipole moment vector and the pump electric field strength vector, δ — Dirac delta function, which was replaced by a Lorentz spectral function in calculations.

For the threshold values of pump emission intensity I_{th}, pump rate W_{th} and inversion n_{th} we obtain expressions with a characteristic dependence of threshold values on field induction $\mathbf{B}$:

$$I_{\text{th}} = \hbar\omega\,\frac{W_{\text{th}}}{\sigma(\mathbf{B})} = \hbar\omega\,\frac{(n_0 + n_{\text{th}})}{(n_0 - n_{\text{th}})}\,\frac{[w_{\text{sp}}(\mathbf{r}_0|\mathbf{B}) + U(\mathbf{r}_0|\mathbf{B})]}{\sigma(\mathbf{B})}, \quad (8)$$

$$W_{\text{th}} = \frac{n_0 + n_{\text{th}}}{n_0 - n_{\text{th}}}\,\frac{1}{T_1}, \quad (9)$$

$$n_{\text{th}} = n_{\text{st}} = 2\kappa/(bV_a). \quad (10)$$

Discussion of Calculation Results

In performing the calculations, the following initial parameter values of the system were used: $\omega_p = 13.87 \cdot 10^{15}\,\text{s}^{-1}$, $\omega_0 = 5.3 \cdot 10^{15}\,\text{s}^{-1}$, $\omega = 5.3585 \cdot 10^{15}\,\text{s}^{-1}$, $\gamma = 1.6 \cdot 10^{11}\,\text{s}^{-1}$, $R = 10\,\text{nm}$, $r_0 = R + 3\,\text{nm}$, $p = 10\,\text{D}$, $\varepsilon_2 = 1.5$, $\varepsilon_\infty = 3.7$, $\kappa = 4.24 \cdot 10^{14}\,\text{s}^{-1}$, $n_0 = 10^{14}\,\text{cm}^{-3}$, $V = 0.0054\,\text{cm}^3$, $V_a = 0.001\,\text{cm}^3$, $I = 1.5 \cdot 10^{16}\,\text{erg/(s·cm}^2)$. Vectors $\mathbf{B}$ and $\mathbf{r}_0$ are collinear with axis Z, while the molecule transition dipole moment vector $\mathbf{p}$ is directed perpendicular to these vectors along axis X. Values of quantities varied during calculations are additionally specified in figure captions.

To investigate the influence of the magnetic field on the dye lasing threshold, it was necessary to reduce the electron collision frequency by three orders of magnitude relative to the characteristic value for noble metals, which is $\gamma = 1.6 \cdot 10^{14}\,\text{s}^{-1}$ at temperature $T \approx 300\,\text{K}$. Methods for reducing the metal NP dissipation parameter were discussed in detail in [33]. With such changes, the spectrum amplitude increases by approximately a factor of 10^5.

As shown previously [31], an external magnetic field affects the magnitude of the transfer rate U and spontaneous emission rate w_{sp}, as well as their resonant frequency. In the presence of a magnetic field, the spectral curve deforms, initially decreasing in amplitude and then splitting into two components. The distance between these components increases with increasing magnetic field induction. For the system under consideration with the constant values specified above, the external exciting field frequency is $\omega = \omega_{\text{res}} = 5.3585 \cdot 10^{15}\,\text{s}^{-1}$, determined based on the analysis of U and w_{sp} spectra.

The dependence of threshold values on the external magnetic field was calculated using formulas (8)–(10). The character of curve changes depends on the exciting field frequency ω (Fig. 5). Fig. 5, *a* shows the magnetic dependence at an exciting field frequency of $\omega = 5.3585 \cdot 10^{15}\,\text{s}^{-1}$. It can be seen that the threshold values of pump emission intensity I_{th} and inversion n_{th} monotonically increase with increasing induction B. The pump threshold W_{th} remains nearly unchanged at low B values, but at $B = 1\,\text{T}$ and above, a sharp decrease in the threshold is observed. Upon deviation from the resonant frequency ω_{res} by thousandths of a percent, the threshold value dependence graph changes (Fig. 5, *b*). The threshold values of pump emission intensity I_{th} and inversion n_{th} decrease with increasing magnetic field induction from 0 to 9 T, after which they begin to increase. For the pump threshold W_{th} the dependence is reversed.

Thus, by selecting certain values of magnetic field induction B and frequency ω it is possible to control the dye lasing threshold.

The influence of the distance r_0 between the molecule and NP on the lasing threshold values was analyzed during the study. It was also found that the concentration of molecules n_0 affects the distance dependence. At relatively low molecule concentrations, the threshold intensity and population inversion increase with increasing distance (Fig. 6, *a*).

At higher molecule concentrations (Fig. 6, *b*), a different character of curve changes is observed. In particular, upon increasing the distance to 20 nm, the intensityI_{th} remains nearly unchanged. However, upon further increase in r_0 the threshold intensity value I_{th} decreases. In contrast, the population inversion exhibits the opposite dependence. From Figs. 6, *a, b*, it also follows that the greater the distance r_0, the lower the threshold pump rate value.

Agreement between the theoretical model and experimental data is achieved by using parameters in calculations that correspond to the real system. In particular, plasma frequency and electron collision frequency values characteristic of silver were used in calculations, which directly correlates with the silver NP employed in experiments.

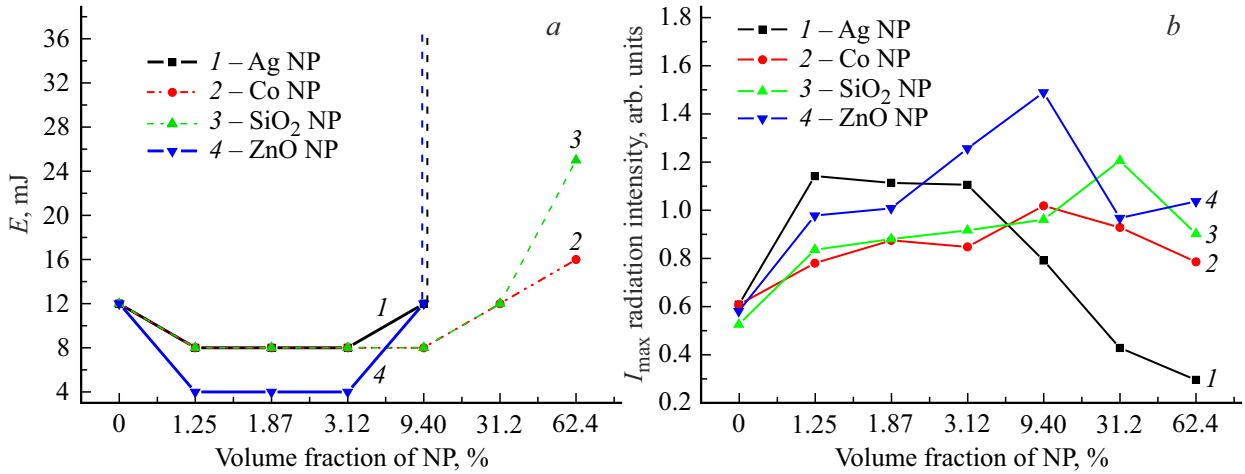

Figure 4. Dependence of lasing threshold (*a*) and glow intensity maximum (*b*) of aqueous R6G solution on NP volume fraction. *1* — Ag, *2* — Co, *3* — SiO_2, *4* — ZnO. Vertical dashed lines indicate cessation of lasing, with the spectrum reverting to the classical form of spontaneous emission.

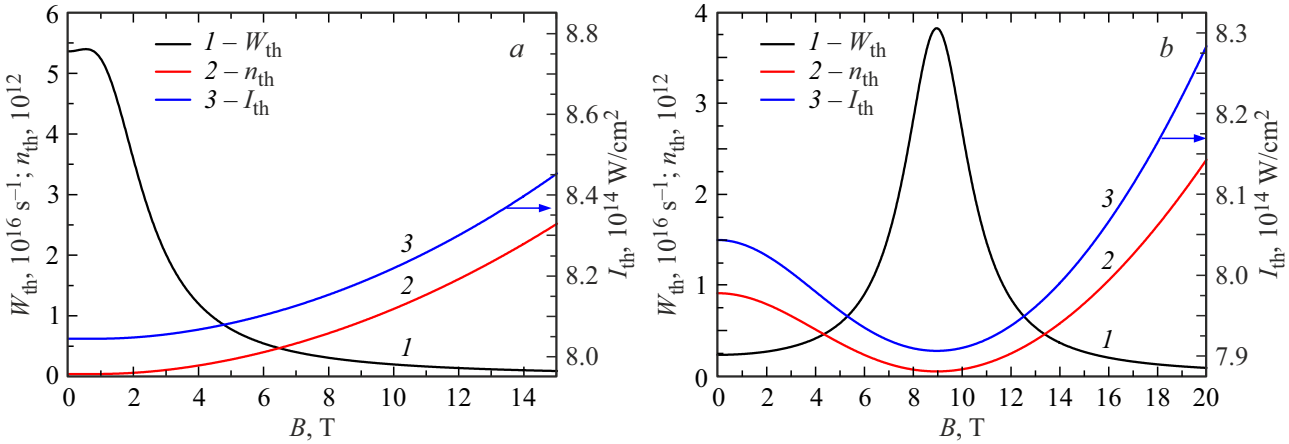

Figure 5. Dependence of dye lasing threshold values on external magnetic field induction: *a* — $\omega = 5.3585 \cdot 10^{15}\,\mathrm{s}^{-1}$, *b* — $\omega = 5.358 \cdot 10^{15}\,\mathrm{s}^{-1}$. *1* — W_{th}, *2* — n_{th}, *3* — I_{th}.

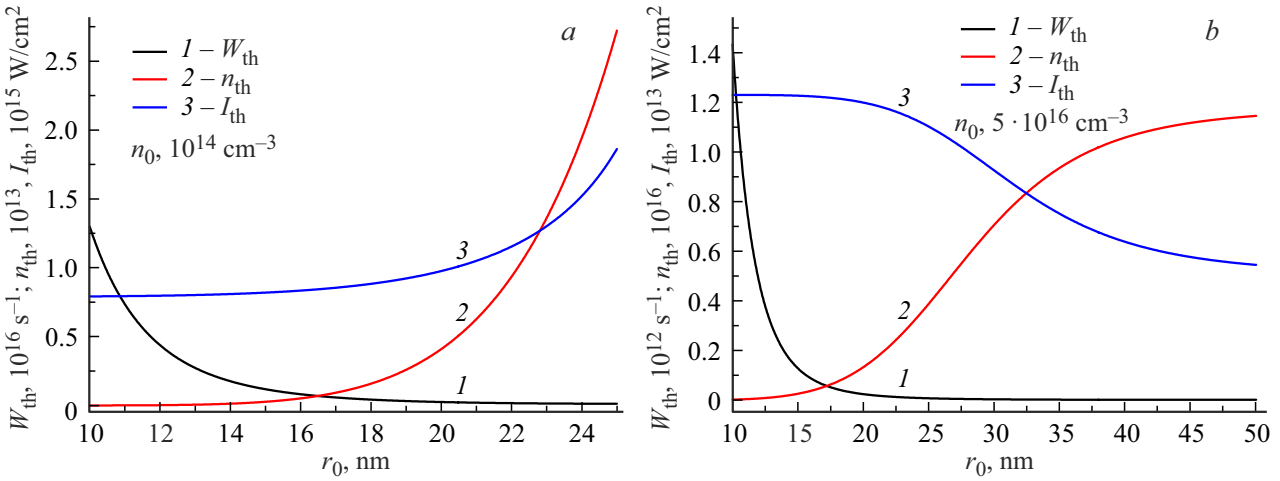

Figure 6. Dependence of dye lasing threshold values on the distance between NP and molecule, $B = 2$ T: *a* — $n_0 = 10^{14}\,\mathrm{cm}^{-3}$, *b* — $n_0 = 5 \cdot 10^{16}\,\mathrm{cm}^{-3}$. *1* — W_{th}, *2* — n_{th}, *3* — I_{th}.

The effect of magnetic field influence on the lasing threshold was not detected in experiments with inductions of 250–300 mT. This is explained by the fact that, as calculations showed, for a visible manifestation of the effect, a magnetic field induction exceeding 1 T and cryogenic cooling (~ 100 K) are required, which could not be provided by the experimental setup used. Thus, these experimental results lay the foundation for future studies using stronger magnetic fields.

Conclusion

In the experimental study of the influence of NP of various materials on the lasing threshold of an aqueous Rhodamine 6G solution, it was established that increasing the NP volume fraction in the solution leads to a reduction in the dye lasing threshold up to a certain limit, after which it increases. This pattern holds for all types of NP. The reduction in lasing threshold is explained by the simultaneous action of the plasmonic mechanism and the „random laser" effect in the solution. A method for experimental detection of the dependence of laser generation characteristics on an external magnetic field is being developed.

Based on the developed theoretical model of laser generation in systems with metallic NP in an active medium, calculations of threshold values of emission intensity I_{th}, pump rate W_{th} and population inversion n_{th} were performed. It was shown that by selecting certain values of constant magnetic field induction B the dye lasing threshold parameters can be varied. The dependence of threshold values on the distance between NP and molecule was also investigated.

The obtained results may be in demand in the development of dye lasers, where a constant magnetic field will be used as an additional external factor for modulating laser emission intensity.

Funding

This study was supported by a grant for conducting major scientific projects in priority areas of scientific and technological development 075-15-2024-550.

Conflict of interest

The authors declare that they have no conflict of interest.

References

[1] V.M. Markushev, M.V. Ryzhkov, C.M. Briskina. Appl. Phys. B, **84**, 333 (2006). DOI: 10.1007/s00340-006-2273-3
[2] K.R. Devika, M. Joby, F. Francis, C.P. Jinsi, R.C. Issac, S.A. Joseph. In: *IOP Conference Series: Materials Science and Engineering* (IOP Publishing, 2022), vol. 1233, p. 012006. DOI: 10.1088/1757-899X/1233/1/012006
[3] V.M. Markushev, M.V. Ryzhkov, C.M. Briskina. Quantum Electronics, **37** (9), 837 (2007). DOI: 10.1070/QE2007v037n09ABEH013439
[4] S.F. Umanskaya, M.A. Shevchenko, N.V. Tcherniega, A.N. Maresev, A.A. Matrokhin, M.A. Karpov, V.V. Voronova. J. Russian Laser Research, **44** (6), 691 (2023). DOI: 10.1007/s10946-023-10179-x
[5] M.S. Hosseini, E. Yazdani, B. Sajad, F. Mehradnia. J. Lumin., **232**, 117863 (2021). DOI: 10.1016/j.jlumin.2020.117863
[6] L. Ye, Y. Feng, C. Lu, G. Hu, Y. Cui. Laser Phys. Lett., **13** (10), 105002 (2016). DOI: 10.1088/1612-2011/13/10/105002
[7] A.M. Brito-Silva, A. Galembeck, A.S.L. Gomes, A.J. Jesus-Silva, C.B. de Araújo. J. Appl. Phys., **108** (3), 033508 (2010). DOI: 10.1063/1.3462443
[8] V.A. Kharenkov, A.Y. Iskandarov, I.A. Edreev. In: *14th International Conference of Young Specialists on Micro/Nanotechnologies and Electron Devices* (IEEE, Novosibirsk, Russia, 2013), p. 198. DOI: 10.1109/EDM.2013.6641974
[9] E.J. Villar, V. Mestre, N.U. Wetter, G.F. de Sá. In: *SPIE OPTO Complex Light and Optical Forces XII* (SPIE, San Francisco, California, United States, 2018), vol. 10549, p. 37. DOI: 10.1117/12.2289228
[10] M.F. Haddawi, J.M. Jassim, S.M. Hamidi. J. Optics, **53** (2), 876 (2024). DOI: 10.1007/s12596-023-01315-6
[11] Z. Wang, X. Meng, A.V. Kildishev, A. Boltasseva, V.M. Shalaev. Laser & Photonics Reviews, **11** (6), 1700212 (2017). DOI: 10.1002/lpor.201700212
[12] W.Z.W. Ismail, J.M. Dawes. Nanomaterials, **12** (4), 607 (2022). DOI: 10.3390/nano12040607
[13] S.F. Haddawi, H.R. Humud, S.M. Hamidi. Optics & Laser Technology, **121**, 105770 (2020). DOI: 10.1016/j.optlastec.2019.105770
[14] J. Tong, S. Li, C. Chen, Y. Fu, F. Cao, L. Niu, T. Zhai, X. Zhang. Polymers, **11** (4), 619 (2019). DOI: 10.3390/polym11040619
[15] L. Salemi, G. Compagnini. J. Laser Appl., **36** (3), 032009 (2024). DOI: 10.2351/7.0001412
[16] V.A. Donchenko, A.A. Zemlyanov, M.M. Zinovjev, A.N. Panamaryova, V.A. Kharenkov. In: *22nd International Symposium on Atmospheric and Ocean Optics: Atmospheric Physics*, ed. by G.G. Matvienko, O.A. Romanovskii. Proc. SPIE (SPIE, San Francisco, California, United States, 2016), vol. 10035, p. 481. DOI: 10.1117/12.2249339
[17] V.A. Donchenko, Al.A. Zemlyanov, M.M. Zinoviev, N.S. Panamarev, A.V. Trifonova, V.A. Kharenkov. Atmospheric and Oceanic Optics, **29**, 452 (2016). DOI: 10.1134/S1024856016050055
[18] V.A. Donchenko, Y.E. Geints, V.A. Kharenkov, A.A. Zemlyanov. Optics and Photonics J., **2013** (3), 13 (2013). DOI: 10.4236/opj.2013.38A002
[19] A.K. Zejnidenov, N.H. Ibraev, M.G. Kucherenko. Vestnik Orenburgskogo gosudarstvennogo universiteta, **9**, 170 (96) (in Russian).
[20] S.N. Smetanin, T.T. Basiev. Quantum Electronics, **43** (1), 63 (2013). DOI: 10.1070/QE2013v043n01ABEH014944
[21] A.L. Burin, M.A. Ratner, H. Cao, R.P.H. Chang. Phys. Rev. Lett., **87** (21), 215503 (2001). DOI: 10.1103/PhysRevLett.87.215503

[22] M.A. Noginov, J. Novak, D. Grigsby, L. Deych. J. Optics A: Pure and Applied Optics, **8** (4), S285 (2006). DOI: 10.1088/1464-4258/8/4/S31
[23] M.G. Kucherenko, V.M. Nalbandyan. J. Appl. Spectrosc., **91** (1), 31 (2024). DOI: 10.1007/s10812-024-01687-y
[24] M.G. Kucherenko, V.M. Nalbandyan, T.M. Chmereva. Opt. Spectrosc., **131** (7), 554 (2023). DOI: 10.1134/S0030400X23050119
[25] S.W. Chang, W.C. Liao, Y.M. Liao, H.I. Lin, H.Y. Lin, W.J. Lin, S.Y. Lin, P. Perumal, G. Haider, C.T. Tai, K.C. Shen, C.H. Chang, Y.F. Huang, T.Y. Lin, Y.F. Chen. Scientific Reports, **8** (1), 2720 (2018). DOI: 10.1038/s41598-018-21228-w
[26] J.S. You, C.F. Hou, Y.C. Chao, Y.C. Tsao, D.N. Feria, T.Y. Lin, Y.F. Chen. APL Materials, **11** (11), 111111 (2023). DOI: 10.1063/5.0173856
[27] S.K. Park, K.D. Kim, H.T. Kim. Colloids and Surfaces A: Physicochemical and Engineering Aspects, **197** (1−3), 7 (2002). DOI: 10.1016/S0927-7757(01)00683-5
[28] H.R. Ghorbani, F.P. Mehr, H. Pazoki, B.M. Rahmani. Orient. J. Chem., **31** (2), 1219 (2015). DOI: 10.13005/ojc/310281
[29] F. Guo, H. Zheng, Z. Yang, Y. Qian. Materials Lett., **56** (6), 906 (2002). DOI: 10.1016/S0167-577X(02)00635-3
[30] M.G. Kucherenko, V.M. Nalbandyan, T.M. Chmereva. J. Opt. Technol., **88** (9), 489 (2021). DOI: 10.1364/JOT.88.000489
[31] M.G. Kucherenko, V.M. Nalbandyan. Materials Today: Proceedings, **71**, 46 (2022). DOI: 10.1016/j.matpr.2022.07.252
[32] Ya.I. Hanin. it Lekcii po kvantovoj radiofizike (IPF RAN, N. Novgorod, 2005). (in Russian).
[33] M.G. Kucherenko, V.M. Nalbandyan. Eurasian Phys. Tech. J., **15** (2 (30)), 49 (2018).

Translated by J.Savelyeva